

Parameter Identification Applied to the Oscillatory Motion of an Airplane Near Stall

James G Batterson*

NASA Langley Research Center Hampton, Virginia

and

Vladislav Klein†

JIAFS/GWU Langley Research Center, Hampton, Virginia

This paper presents an application of a stepwise regression incorporating polynomial splines to oscillatory flight data from a light research airplane operating at near stall angles of attack. It is shown that data from several experiments can be combined into a large data set for analysis and that hysteresis phenomena can be observed in this large data set. Finally, it is postulated from the analysis of the flight data and theoretical calculations that the observed oscillatory motion is the result of a combination of wing stall and wing wake position at the tail.

Nomenclature

a_z	= acceleration along vertical body axis, g
\bar{c}	= mean aerodynamic chord, m
C_L	= lift coefficient
C_m	= pitching moment coefficient
C_{m_q}	$= \partial C_m / [\partial (\dot{q}\bar{c}/2V)]$
C_{m_α}	$= \partial C_m / \partial \alpha$
$C_{m_{\dot{\alpha}}}$	$= \partial C_m / [\partial (\dot{\alpha}\bar{c}/2V)]$
$C_{m_{\delta e}}$	$= \partial C_m / \partial \delta e$
C_z	= vertical force coefficient
C_{z_q}	$= \partial C_z / [\partial (\dot{q}\bar{c}/2V)]$
C_{z_α}	$= \partial C_z / \partial \alpha$
$C_{z_{\dot{\alpha}}}$	$= \partial C_z / [\partial (\dot{\alpha}\bar{c}/2V)]$
$C_{z_{\delta e}}$	$= \partial C_z / \partial \delta e$
F	= statistical F value
F_{crit}	= critical F value
F_p	= partial F value
g	= gravitational constant 9.8 m/s^2
h	= lag number
I_y	= moment of inertia about lateral body axis
K	= number of knots
m	= airplane mass
M	= maximum lag number
$n(i)$	= equation error at i th measurement
N	= number of data points
q	= pitch rate, rad/s
Q	= number of terms in model
s^2	= sample variance
S	= wing area m^2
t	= time, s
V	= airspeed m/s
W	= autocorrelation function
x_i	= independent variable
y	= dependent variable
α	= angle of attack deg or rad
α_i	= value of i th knot in angle of attack deg or rad
δe	= stabilator deflection deg or rad
ϵ	= downwash angle at tail deg
θ_i	= parameter associated with independent variable x_i
$\nu(i)$	= residual at i th measurement
ρ	= atmospheric density
σ	= population standard error

Superscripts

$(\dot{})$	= differentiation with respect to time
$(\hat{})$	= estimated value

Introduction

ALTHOUGH techniques for the stability and control analysis of airplanes from flight data limited to the linear flight regimes are well known and documented, the analysis of flight data from nonlinear flight regimes is a subject of current study.^{1,3} In this paper, flight data recorded during seemingly spontaneous longitudinal oscillations of a light research airplane operating near stall angle of attack are analyzed. An example of these oscillations is presented in Fig. 1 where they comprise a steady residual oscillation after the initial response to an input dies out. Such oscillatory motion has popularly been referred to as "bucking" or "porpoising." Phillips⁴ has proposed several different aerodynamic models for this behavior and tested those models on a hybrid computer. Hence, the usual parameter estimation problem at low angles of attack now becomes twofold at high angle of attack. The first part of the problem is to determine the aerodynamic model structure or form. Once this structure has been postulated, then one may estimate the corresponding stability and control parameters. Stepwise regression is chosen for the model structure determination and parameter estimation. This equation error formulation builds an aerodynamic model based on a user postulated set of candidate variables. At each step of the model building, a linear regression estimate of the included stability and control parameters is made.

First, this paper will present a synopsis of the stepwise regression technique used for the data analysis. Both the acquisition of the data and the results of applying the stepwise regression to that oscillatory flight data will be discussed. The fourth part of this paper will present a physical interpretation of the observed oscillatory behavior based on the results of the analysis and theoretical considerations. A concluding section will summarize the results and provide ideas for further investigation.

Airplane Identification Using Stepwise Regression

The general form of aerodynamic model equations can be written as

$$y(t) = \theta_0 + \theta_1 x_1 + \dots + \theta_{Q-1} x_{Q-1} \quad (1)$$

Received Sept. 5, 1983; revision received Feb. 6, 1984. This paper is declared a work of the U.S. Government and therefore is in the public domain.

*Aero Space Technologist, Member AIAA.

†Research Professor, Associate Fellow AIAA.

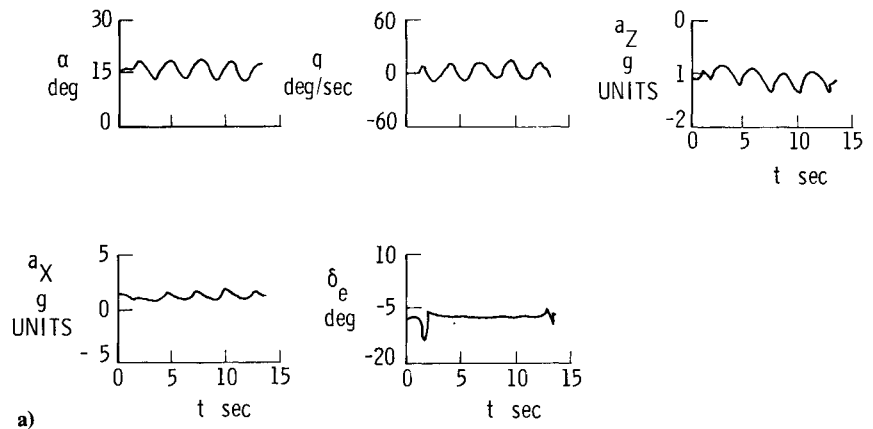
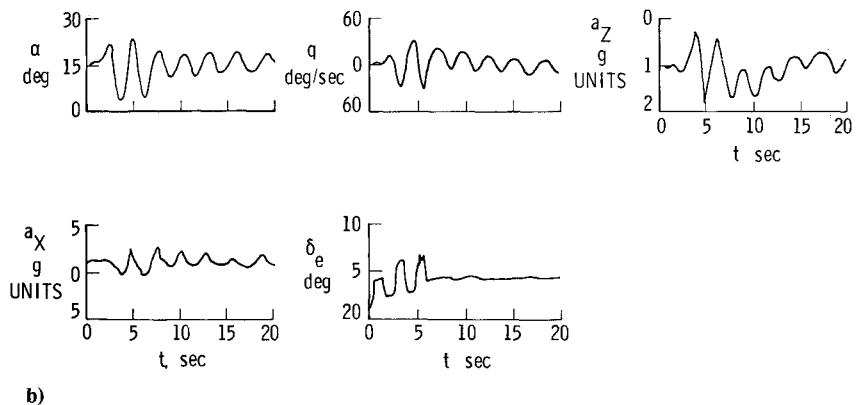


Fig 1 Time histories of selected longitudinal variables from two representative oscillatory runs



In this equation, $y(t)$ represents the resultant coefficient of aerodynamic force or moment (the dependent variable), θ_0 to θ_{Q-1} are the constant coefficients in a polynomial spline representation of the aerodynamic functions, and x_1 to x_{Q-1} are the airplane response and input variables and their combinations (the independent variables). When the aerodynamic model equations are postulated, the determination of significant terms among the candidate variables (determination of the model structure) and estimation of corresponding parameters follow.

Assuming that a sequence of N observations of y and x at times t_1, t_2, \dots, t_N have been made, the measured values denoted by $y(i)$ and $x(i)$ where $i=1, 2, \dots, N$ are related by the following set of N linear equations:

$$y(i) = \theta_0 + \theta_1 x_1(i) + \dots + \theta_{Q-1} x_{Q-1}(i) + n(i) \quad (2)$$

where $n(i)$ represents the equation error. An adequate model for the aerodynamic coefficients can be determined by applying the stepwise regression.⁵

This procedure begins with the assumption that there are no variables in the postulated regression equation other than the bias term θ_0 . An effort is then made to find an optimal subset of variables by inserting independent variables into the model one at a time. The first independent variable selected for entry into the equation is the one that has the largest correlation with the dependent variable y . Suppose that this variable is x_1 . This is also the variable that produces the largest value of the F statistic for testing the significance of regression. The variable is entered if the partial F statistic F_P exceeds a preselected critical F value, i.e.,

$$F_P = \frac{\hat{\theta}_1^2}{s^2(\hat{\theta}_1)} > F_{\text{crit}} \quad (3)$$

where θ_1 is the estimated parameter associated with x_1 and $s^2(\hat{\theta}_1)$ is the variance estimate of $\hat{\theta}_1$.

The second variable chosen for entry is the one that now has the largest correlation with y after adjusting for the effect of the first variable entered (x_1 in this case) on y . These correlations are referred to as partial correlations. In general, at each step, the independent variable having the highest partial correlation with y is added to the model only if its partial F statistic exceeds the preselected F_{crit} . At each step of the procedure, all variables previously entered into the model are also reassessed by reevaluating and examining their partial F statistics. A variable added at an earlier step may become redundant because the relationship between it and the remaining variables now in the equation has reduced its value of F_P to less than F_{crit} . If this happens the insignificant variable is deleted from the regression model. The procedure terminates when all significant terms have been included in the model.

Several quantities indicating "goodness of fit" or model adequacy are calculated at each stage of the stepwise regression as each new variable enters the model. All of these quantities should be examined for the final model selection. Other criteria such as the Akaike criterion and Mallows C_p have been examined in the past. However, the criteria presented here have the desirable properties of not requiring a priori variance estimates and/or time propagation of the estimates. This allows one to combine several sets of data into one large set or to combine several subsets of data from separate experiments into one set for analysis. First, the user can consider the total F value for a given model of Q variables, calculated as the ratio of the mean square due to the regression to the mean square of the residual.

This ratio is given as

$$F = \sum_{i=1}^N [\hat{y}(i) - \bar{y}]^2 / \sum_{i=1}^N [y(i) - \hat{y}(i)]^2 \quad \left(\frac{N-Q}{Q-1} \right) \quad (4)$$

where

$$\bar{y} = \frac{1}{N} \sum_{i=1}^N y(i)$$

This number usually increases to some maximum value as new variables enter the regression, but then decreases slightly as the new terms are less effective in reducing the residuals. Heuristically the maximum F value represents a model which best fits the data with a minimum number of parameters. Second, the squared multiple correlation coefficient R^2 is considered. This number expressed as a percentage, is a measure of the usefulness of the terms other than θ_0 in the model. The value of R^2 would be 100% for a model that fit the data perfectly. Third, at each stage, the partial F values F_p , for each parameter are examined. One should look for consistency in the values of F_p . For example, if one value of F_p is only slightly greater than F_{crit} while all other values of F_p are much greater, one may not want to include the variable with the small value of F_p in the model. The fourth aid in model selection is the estimated normalized autocorrelation function for the residuals. An estimate of the autocorrelation function at lag h is given by

$$W(h) = \frac{1}{N-h} \sum_{i=1}^{N-h} v(i)v(i+h) \quad h=0, 1, \dots, M \quad (5)$$

where h is the lag number and M is the maximum lag number, which is usually 10% of N . The normalized autocorrelation function is calculated as $W(h)/W(0)$. This function should approach that for white noise with a value of 1 at zero lag and values of 0 at lags of 1 to M . In applications, when the value of F_p for a parameter makes the utility of an independent variable questionable, the contribution of that variable to the actual model structure can be assessed by observing the effect of the variable on the autocorrelation function of the residuals. A fifth number that facilitates model selection is the standard error in the residuals s which is calculated at each stage of the regression.

One learns from experience that not all of the five criteria listed above are "optimally" satisfied for any single model. However the stepwise regression and its associated information criteria do significantly reduce the number of possible models from which one must choose. Moreover as the model structure is determined, so are the parameter estimates. Finally, the ambiguity in the model selection can also be resolved by requiring that the estimated parameters make sense physically and that the selected model has good prediction capability.

The independent variables have been postulated in the form of polynomial splines as a function of angle of attack. This formulation allows for different values of stability and control parameters to be estimated for different values of angle of attack. The spline approach is more general than the simple polynomial expansion of the aerodynamic function¹ and can be described as follows. The range of the independent variable that is most important in the determination of the dependent variable is partitioned into several subsets, each having support on less of the range than the previous subset. For example, the force coefficient C_z is mainly dependent on α . Hence, if $\alpha = \{z | a < z < b\}$, then the α range, $[a, b]$, is divided according to the spline basis functions as follows:

$$\begin{aligned} (\alpha - \alpha_i)_+^m &\equiv (\alpha - \alpha_i)^m & (\alpha \geq \alpha_i) \\ &\equiv 0 & (\alpha < \alpha_i) \end{aligned} \quad (6)$$

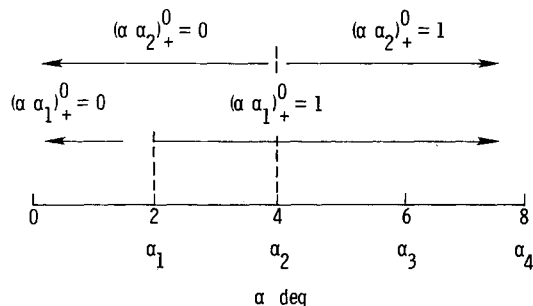


Fig 2 Illustration of regions of support for spline basis functions

The values of α_i are called knots. An example of the "+" function is given in Fig 2. The four knots in this figure are at $\alpha = 2, 4, 6,$ and 8 deg. Hence, $(\alpha - \alpha_1)_+^0 = 1$ for $\alpha \geq \alpha_1 = 2$ deg, and $(\alpha - \alpha_1)_+^0 = 0$ for $\alpha < \alpha_1$. Similarly, $(\alpha - \alpha_2)_+^0 = 1$ for $\alpha \geq 4$ deg and $(\alpha - \alpha_2)_+^0 = 0$ for $\alpha < 4$ deg and so forth, for the rest of the "+" functions. If the order of the "+" function, denoted by the superscript m , is other than zero, say 2, then,

$$\begin{aligned} (\alpha - \alpha_i)_+^2 &= (\alpha - \alpha_i)^2 & \text{for } \alpha \geq \alpha_i \\ &= 0 & \text{for } \alpha < \alpha_i \end{aligned}$$

For the analysis in this paper the knots were placed every 0.5 deg between $\alpha = 9$ and 18 deg, and the equations of motion were formulated as

$$\frac{2mg}{\rho V^2 S} a_z = C'_z(\alpha) + C'_{z_q}(\alpha) \frac{q\bar{c}}{2V} + C_{z_{\delta e}}(\alpha) \delta e \quad (7)$$

$$\frac{2I_y}{\rho V^2 S \bar{c}} \dot{q} = C_m(\alpha) + C_{m_q}(\alpha) \frac{q\bar{c}}{2V} + C_{m_{\delta e}}(\alpha) \delta e \quad (8)$$

where

$$C_z(\alpha) = C_{z_0} + C_{z_\alpha} \alpha + \sum_{i=1}^K C_{z_{\alpha_i}} (\alpha - \alpha_i)_+ \quad (9)$$

$$C'_{z_q}(\alpha) = C'_{z_q} + \sum_{i=1}^K C'_{z_{q_i}} (\alpha - \alpha_i)_+^0 \quad (10)$$

$$C_{z_{\delta e}} = C_{z_{\delta e}} \delta e + \sum_{i=1}^K C_{z_{\delta e_i}} (\alpha - \alpha_i)_+^0 \quad (11)$$

$$C_m(\alpha) = C_{m_0} + C_{m_\alpha} \alpha + \sum_{i=1}^K C_{m_{\alpha_i}} (\alpha - \alpha_i)_+ \quad (12)$$

$$C'_{m_q}(\alpha) = C'_{m_q} + \sum_{i=1}^K C_{m_{q_i}} (\alpha - \alpha_i)_+^0 \quad (13)$$

$$C_{m_{\delta e}}(\alpha) = C_{m_{\delta e}} \delta e + \sum_{i=1}^K C_{m_{\delta e_i}} (\alpha - \alpha_i)_+^0 \quad (14)$$

and the prime notation indicates the following relation

$$C'_{z_q} = C_{z_q} + C_{z_{\dot{\alpha}}} \quad (15)$$

$$C'_{m_\alpha} = C_{m_\alpha} + \frac{\rho S \bar{c}}{4m} C_{m_{\dot{\alpha}}} C_{z_\alpha} \quad (16)$$

$$C_{m_q} \doteq C_{m_q} + C_{m_{\dot{\alpha}}} \quad (17)$$

$$C_{m_{\delta e}} \doteq C_{m_{\delta e}} \quad (18)$$

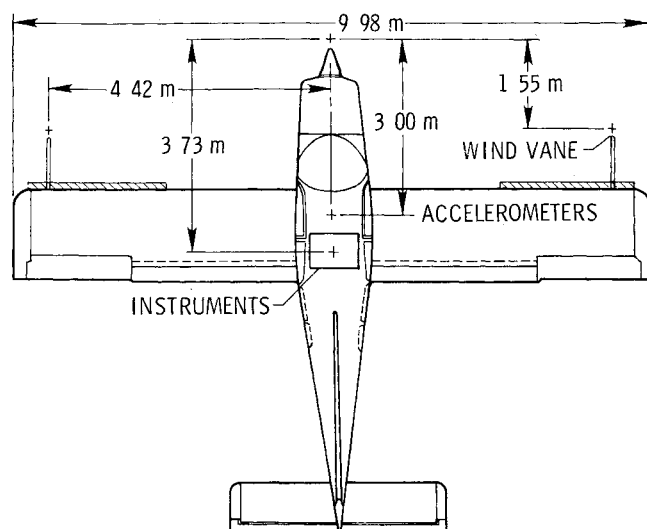


Fig 3 Top view drawing of test airplane showing wing outboard leading edge modifications (not to scale)

Low degree splines are used to give insight to the physics of the phenomenon being analyzed. After the relevant knots have been discovered, refinements (smoothing) of the polygonal lines representing the derivatives can be achieved by judiciously incorporating higher degree splines.²

Flight Vehicle and Data Acquisition

The test flight vehicle was a single engine, low wing, four seat, light airplane. Flight control was provided by the throttle, stabilator (all movable tail), ailerons, and rudder. Flaps were available but were not used in the tests considered in this report. The wing leading edge had been modified by extending the outboard half of each leading edge as indicated in Fig 3. This was one of several leading edge modifications that were made on this airplane to study the stall/spin characteristics of such a modified airplane. The flight data analyzed herein were obtained during standard stability and control parameter estimation flights. In these flights the pilot attempts to trim the airplane to some steady state reference flight condition from which he can initiate some perturbation by the movement of controls. All data analyzed in this report are assumed to have equilibrium initial conditions ($p=q=r=\dot{\alpha}=\dot{\beta}=\dot{\gamma}=\dot{v}=\dot{w}=\dot{u}=0$). Data were measured by rate gyros for roll, pitch, and yaw rates; roll and pitch angles were measured by attitude gyros. Angles of attack and sideslip were measured by wind vanes mounted on booms on each wing tip, as shown in Fig 3. Linear accelerations were measured by accelerometers located close to the airplane center of gravity (c.g.) with three mutually orthogonal axes pointing in the directions of the longitudinal, lateral, and vertical body reference axes of the airplane. Control displacements were measured by potentiometers located close to the respective control surfaces to eliminate time delays and inaccuracies in the measurements of displacements due to control cable stretch.

Data were recorded onboard the test airplane as analog voltage signals. The records of these voltages were filtered by a 6 Hz low pass filter and digitized to a sample rate of 20/s after each flight. The digitized 20 sample per second data were then corrected for c.g. offset of the instruments, upwash and bias error on the wind vanes, and bias errors in the a_z accelerometer and the angular rate gyros.

Data Analysis

The stepwise regression first was applied to each of the 11 oscillatory runs. Time histories of selected longitudinal

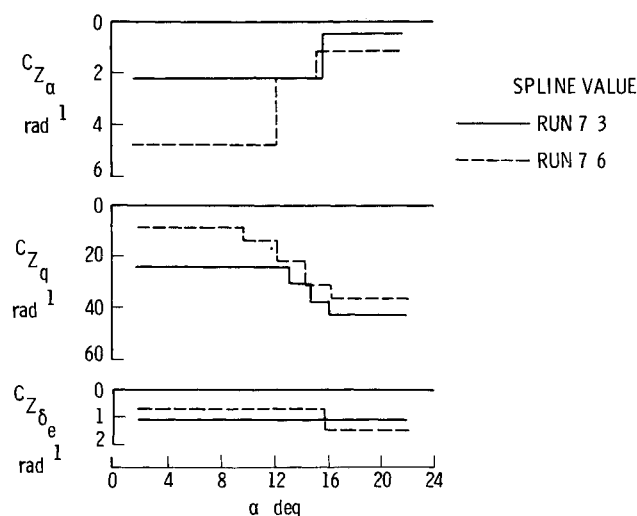


Fig 4a Z force coefficients from runs 7 3 and 7 6

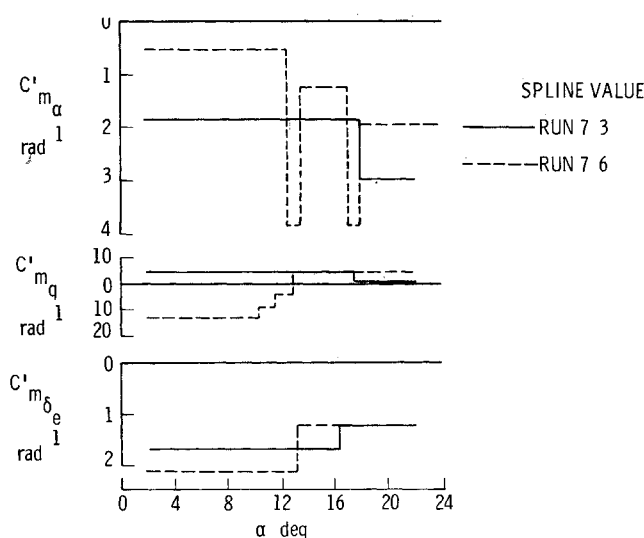


Fig 4b Pitching moment coefficients from runs 7 3 and 7 6

variables for two typical runs are presented in Fig 1. Here run 7 3 shows the development of an oscillation after a stabilator pulse and run 7 6 shows the development of a similar oscillation after a strong stabilator doublet. The application of the stepwise regression with knots at every 0.5 deg in α for α between 9 and 18 deg to these two runs yielded the stability and control derivatives plotted in Fig 4. From C_{Z_α} it is seen that the lift curve slope starts to "flatten" at $\alpha=12$ deg and flattens even more at $\alpha=16$ deg. Moreover, C_{Z_q} becomes a strong influence as the angle of attack progresses from 12 to 17 deg. The pitching moment coefficient analysis indicates a stall possibly at 12 deg, but surely by 16 deg angle of attack where C_{m_α} decreases to values around -4. C_{m_q} becomes positive around $\alpha=12$ deg, indicating a loss of pitch damping. Hence, by incorporating the spline basis into a stepwise regression algorithm, one can realize good approximations to aerodynamic coefficients that are nonlinear over the angle of attack range of the flight. Still, as seen by the analysis of the two runs above, there is some inconsistency in the results. To improve on these results, C_X , C_Z , and C_m were calculated for each point in each of the 11 runs. Next, all 11 runs were combined to create one large data set of approximately 3000 points. Then this large set was analyzed as three sets of 1000 points each. The results of the analysis of one of these sets are

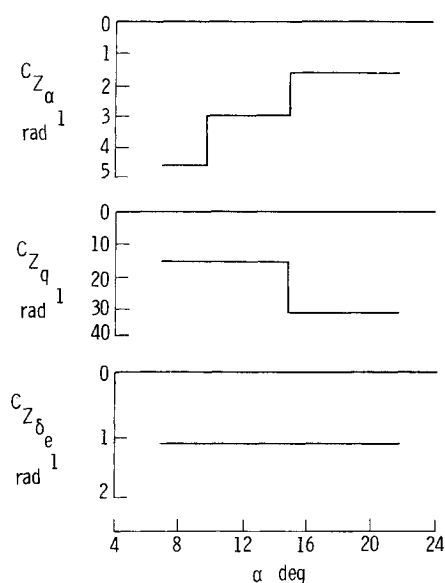


Fig 5a Z force coefficients from combined data set

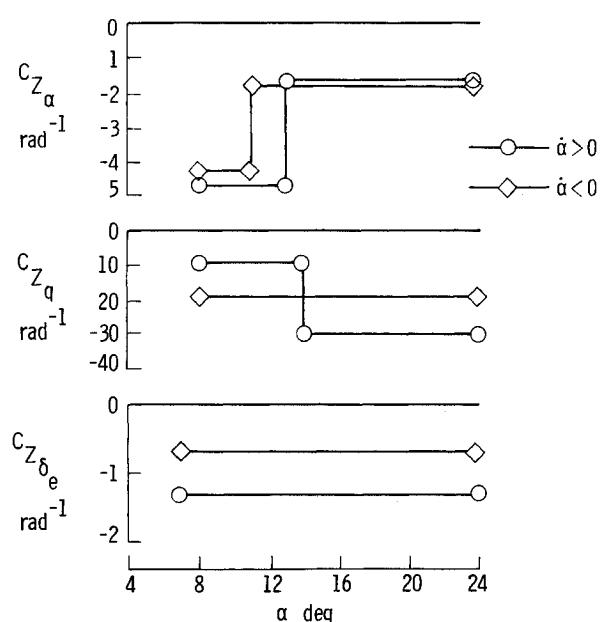
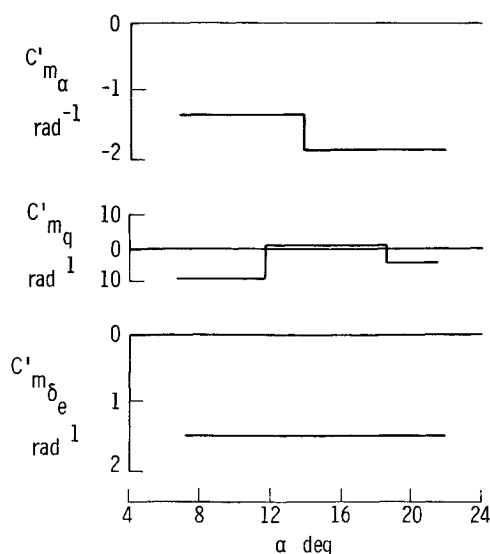
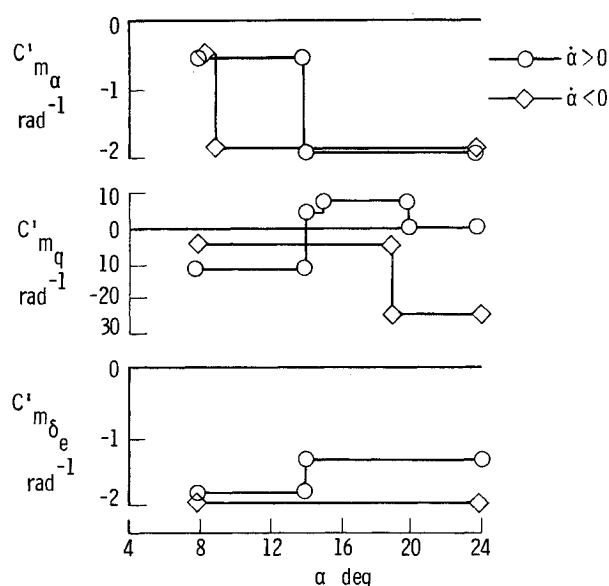
Fig 6a Z force coefficients from combined data set analyzed separately for $\dot{\alpha} > 0$ and $\dot{\alpha} < 0$ 

Fig 5b Pitching moment coefficients from combined data set

Fig 6b Pitching moment coefficients from combined data set analyzed separately for $\dot{\alpha} > 0$ and $\dot{\alpha} < 0$

given in Fig 5. These results agree well with the analysis of the individual runs.

The possibility of hysteresis (dependence of aerodynamics on the sign of $\dot{\alpha}$) was examined by applying the stepwise regression to each of the 1000 point data sets in two parts. In the first part only data corresponding to $\dot{\alpha} > 0$ were analyzed while in the second part only data occurring with $\dot{\alpha} < 0$ were analyzed. The results of these analyses are presented in Fig 6. Here some obvious $\dot{\alpha}$ effects are seen. For example, the flattening of the lift curve is delayed until $\alpha = 13$ deg for $\dot{\alpha} > 0$, while $C_{Z_\alpha} = -1.6$ down to $\alpha = 9$ deg for decreasing angle of attack. C_{Z_q} only becomes a strong influence for increasing angle of attack. The sharp negative increase in pitching moment at $\alpha = 14$ deg only occurs for $\dot{\alpha} > 0$. Finally the positive C_{m_q} is limited to $\dot{\alpha} > 0$ in the $\alpha > 15$ deg range. To further assess the existence of hysteresis in the lift curve $C_L = -C_Z$ was plotted using the estimated parameters from all of the large data sets. The results are presented in Fig 7. The consistency with which $C_L(\dot{\alpha} > 0)$ exceeds $C_L(\dot{\alpha} < 0)$ leads to the conclusion that hysteresis does exist in the lift curve. The possibility of such hysteresis was tentatively identified in the analysis of a quasisteady maneuver of the same airplane.¹

Interpretation of Results

The estimated values of the stability and control derivatives suggest several mechanisms are responsible for the observed aerodynamic behavior. Because of the limited number of measured response variables and correlation among those variables it is not always possible to separate certain effects which influence airplane motion. For example, in the present experiment, there is no information on the aerodynamics at the horizontal tail or on the separate effects of q and $\dot{\alpha}$. These two variables are almost linearly correlated as is apparent from their time histories presented in Fig 8.

The effect on damping in pitch is through the derivatives $C_{m_{\dot{\alpha}}}$ and C_{m_q} , where the latter term is proportional to change in downwash angle at the tail $\partial\epsilon/\partial\alpha$. Normally, $\partial\epsilon/\partial\alpha$ is constant for low angles of attack. However, $\partial\epsilon/\partial\alpha$ can change sign near the wing stall angle of attack due to a decrease in lift

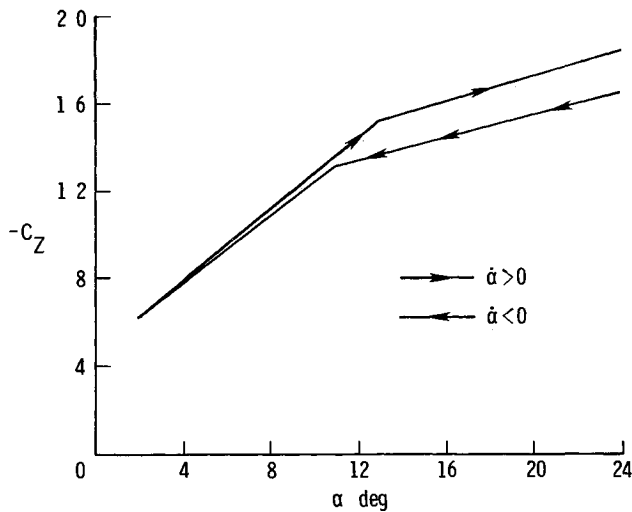


Fig 7 Lift curve approximated from combined data set indicating hysteresis

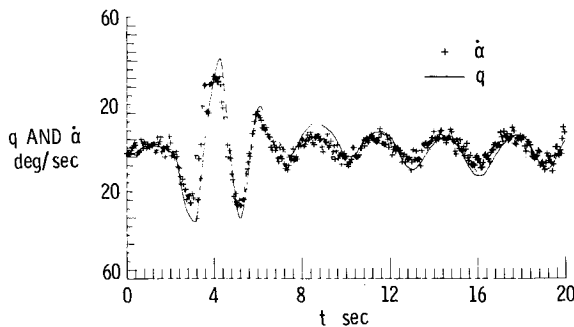


Fig 8 Time histories of pitch rate and rate of change of angle of attack for an oscillatory run

with increasing angle of attack (post stall) or due to the upward shift of the wing wake behind the stalled or partially stalled airfoil.⁶

Theoretical calculations for ϵ and $\partial\epsilon/\partial\alpha$ can be made using the methods of Silverstein et al.⁶ Calculations for the values of q and $\dot{\alpha}$ derivatives as functions of $\partial\epsilon/\partial\alpha$ can be made from Etkin⁷ [note sign error in Eqs (7-10) and (11) in Ref 7]. The results of these calculations are presented in Fig 9. It is seen that $C_{Z_{\dot{\alpha}}}$ must exhibit the same trend as $C_{m_{\dot{\alpha}}}$. Hence, if C_{m_q} is driven to zero by its C_m component, then C'_{Z_q} should be similarly affected by $C_{Z_{\dot{\alpha}}}$ at the tail. However, C'_{Z_q} actually becomes quite pronounced at angles of attack where C_{m_q} is near zero (Figs 4-6). This apparent inconsistency can be explained through the mechanism of dynamic stall.^{4,8,9} Through this mechanism the wing makes a greater contribution to C'_{Z_q} (which combines C'_{Z_q} and $C_{Z_{\dot{\alpha}}}$) than the tail. Although the experimental data are sparse, Phillips⁴ used an envelope that allows for a $C_{Z_{\dot{\alpha}}}$ component of -20 .

Therefore, one explanation of the airplane motion is as follows: The airplane is trimmed near $\alpha = 14$ deg. To ascertain the stability of the trim conditions a "variance" of the stabilator from trim was calculated. This calculation was performed by summing the squares of the differences between stabilator setting and trim setting for 10 data points (0.5 s) before and 10 data points after the pilot indicated the airplane to be trimmed. For $\alpha < 13$ deg and $\alpha > 18$ deg this variance was very small, but for $13 \text{ deg} < \alpha < 18 \text{ deg}$ large variations were found as seen in Fig 10. In Fig 10, the error bars outside the [13-18 deg] angle of attack region are within the symbol. Hence it is seen that a trim at $\alpha = 14$ deg is not very stable. The flow on the rear portion of the inboard half of each wing

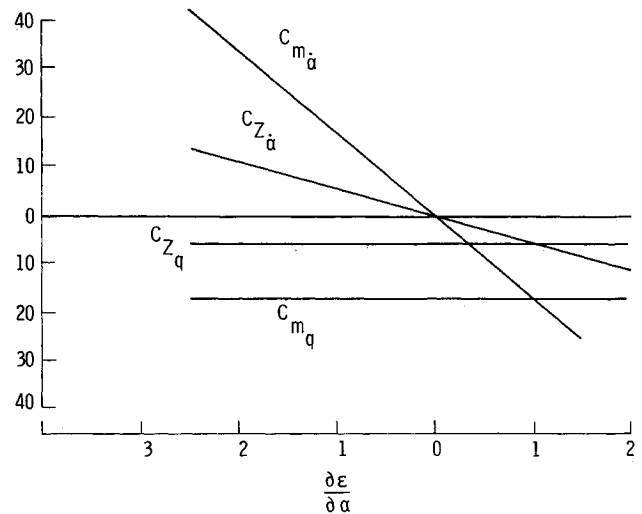


Fig 9 Tail contribution (semiempirical) to q and $\dot{\alpha}$ derivatives

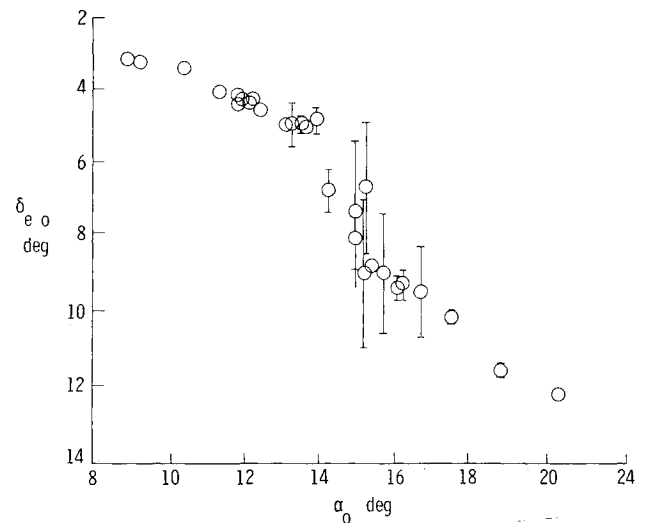


Fig 10 Stabilator trim deflection plotted against angle-of attack trim curve showing uncertainty in stabilator displacement required for trim between $\alpha = 14$ and 18 deg

(basic airfoil part) is separated. The turbulent boundary layer allows for the delay of actual stall on this section as long as the pitching motion of the airplane is somewhat benign. However, the origin of the wake from this section is shifted upward from the trailing edge. The wake now passes just below the stabilator which is set at -5 deg and has previously experienced downwash angles of about 7 deg leaving the tail angle of attack at about 2 deg. A nose up pulse from the stabilator then sends the tail into the wing wake. This rotation also gives rise to a shedding of a leading edge vortex when the wing is past its static stall angle of attack. The trailing edge separation then encompasses the entire inboard half of the wing and $\partial\epsilon/\partial\alpha$ becomes positive. Hence, there is no pitch damping due to pitch rate. However, there is a negative pitching moment due to the rearward shift of the wing aerodynamic center at the stall of the inboard section. This stall is evident by the negative change in $C_{m_{\dot{\alpha}}}$ at $\alpha = 14$ deg.

It should be noted that moment stall should precede lift stall during the dynamic stall phenomenon.⁷ From Fig. 1, maximum lift corresponds to $\alpha = 16.5$ deg. As the angle of attack decreases at a lower C_L than was in effect during the increase in angle of attack, some pitch damping is evident. As the wing flow reattaches at $\alpha = 12$ deg, the tail is above the

wing wake and set to provide a pitch up moment toward $\alpha = 14$ deg. The downward rotation of the nose is arrested, turned into an upward rotation, and the entire above process repeats itself.

This possible explanation is, of course, only preliminary. A more precise explanation of the motion could be provided by further flight tests with a stabilator mounted α vane and pitot tube to record downwash and wake data. Also, a wind tunnel test in which the individual effects of the wing and tail can be assessed could prove helpful.

Concluding Remarks

This paper has demonstrated the utilization of a stepwise regression with spline basis functions for model structure determination and parameter estimation from flight data in which aerodynamic force and moment coefficients are nonlinear functions of state and control variables. By combining several runs it was possible to show hysteresis in the lift curve and some effects of dynamic stall. From the estimated derivatives and theoretical calculations, it was postulated that the oscillatory motion of the airplane is caused by a combination of wing stall and wing wake position at the tail.

The effect of the outboard leading edge modifications prevented a pure or total wing stall and/or roll off, thus ensuring a pure longitudinal oscillation. Planforms which prevent tip stall should be examined for similar behavior with the horizontal tail *in situ*.

Further work is suggested in the wind tunnel where q and α , wing and tail effects might be separated. Also, further flight testing with an α vane mounted just forward of the stabilator

to record downwash data is recommended. Such downwash and wake data could be correlated with wind tunnel pitching moment data to make the latter more useful in the future. Moreover, additional data would allow for the acceptance of the above postulated theory or the development of a better theoretical explanation of the airplane's behavior.

References

- ¹Klein, V. and Batterson, J. G. Determination of Airplane Model Structure from Flight Data Using Splines and Stepwise Regression. NASA TP 2126 March 1983.
- ²Vincent, J. H., Gupta, V. K., and Hall, W. E., Jr. Recent Results in Parameter Identification for High Angle of Attack Stall Regimes. AIAA Paper 79-1640 Aug. 1979.
- ³Maine, R. E. and Iliff, K. W. Formulation and Implementation of a Practical Algorithm for Parameter Estimation with Process and Measurement Noise. *SIAM Journal of Applied Mathematics* Vol. 41, No. 3 Dec. 1981, pp. 558-579.
- ⁴Phillips, W. H. Simulation Study of the Oscillatory Longitudinal Motion of an Airplane at the Stall. NASA TP 1242 1978.
- ⁵Draper, N. R. and Smith, H. *Applied Regression Analysis*. John Wiley and Sons, New York, 1966.
- ⁶Silverstein, A., Katzoff, S., and Bullivant, W. K. Downwash and Wake Behind Plain and Flapped Airfoils. NACA Rept. 651 1939.
- ⁷Etkin, B. *Dynamics of Atmospheric Flight*. John Wiley and Sons, New York, 1972.
- ⁸Ham, N. D. Aerodynamic Loading on a Two Dimensional Airfoil During Dynamic Stall. *AIAA Journal* Vol. 6 Oct. 1968 pp. 1927-1934.
- ⁹McCroskey, W. J. Some Current Research in Unsteady Dynamics. *Transactions of the ASME Journal of Fluids Engineering* Vol. 99, Ser. 1 No. 1 March 1977 pp. 8-38.

From the AIAA Progress in Astronautics and Aeronautics Series

INJECTION AND MIXING IN TURBULENT FLOW—v. 68

By Joseph A. Schetz, Virginia Polytechnic Institute and State University

Turbulent flows involving injection and mixing occur in many engineering situations and in a variety of natural phenomena. Liquid or gaseous fuel injection in jet and rocket engines is of concern to the aerospace engineer; the mechanical engineer must estimate the mixing zone produced by the injection of condenser cooling water into a waterway; the chemical engineer is interested in process mixers and reactors; the civil engineer is involved with the dispersion of pollutants in the atmosphere; and oceanographers and meteorologists are concerned with mixing of fluid masses on a large scale. These are but a few examples of specific physical cases that are encompassed within the scope of this book. The volume is organized to provide a detailed coverage of both the available experimental data and the theoretical prediction methods in current use. The case of a single jet in a coaxial stream is used as a baseline case, and the effects of axial pressure gradient, self-propulsion, swirl, two-phase mixtures, three-dimensional geometry, transverse injection, buoyancy forces, and viscous-inviscid interaction are discussed as variations on the baseline case.

200 pp., 6 × 9 illus. \$17.00 Mem. \$27.00 List

TO ORDER WRITE: Publications Order Dept., AIAA, 1633 Broadway, New York, N.Y. 10019